JOURNAL OF AIRCRAFT
Vol. 36, No. 4, July–August 1999

Toward Cost-Effective Aeroelastic Analysis on Advanced Parallel Computing Systems

S. A. Goodwin*
Lockheed Martin Aeronautical Systems, Marietta, Georgia 30063-0685
R. A. Weed†
Mississippi State University, Vicksburg, Mississippi 39180-5789
L. N. Sankar‡
Georgia Institute of Technology, Atlanta, Georgia 30332-0150
and
P. Raj§
Lockheed Martin Aeronautical Systems, Marietta, Georgia 30063-0685

Progress toward the development and validation of a fast, accurate, and cost-effective aeroelastic method for several advanced parallel computing platforms is presented. The ENSAERO code, developed at NASA Ames Research Center, was selected for this research effort. To improve the performance, the capabilities of the constituent modules have been enhanced. The relative merits of four parallel computing environments are investigated: SGI workstation cluster, SGI Power Challenge machine, SGI Power Challenge cluster, and the IBM SP2 system. To assess the computational performance of the enhanced ENSAERO code, the results of unsteady Navier–Stokes simulations of the transonic flow over a fully flexible aeroelastic arrow-wing body configuration are reported. In addition, to ensure that the modified version of ENSAERO performs to specifications and to evaluate the benefits of the enhancements, unsteady Euler/Navier–Stokes calculations for an AGARD standard aeroelastic configuration are done. To evaluate the level of accuracy of the enhanced system, the ENSAERO results are compared with established computational solutions and experimental data.

Nomenclature

M = Mach number
q = dynamic pressure
Re = Reynolds number based on root chord
α = angle of attack

Introduction

TRANSPORT aircraft of the future are expected to become much more complex than today's aircraft. Their design will require teams of engineers working closely across geographical and organizational boundaries. The U.S. aerospace industry must, therefore, improve the processes and capabilities to meet tomorrow's design challenges by incorporating validated, cost-effective methods into the design process. Using methods that provide improved understanding of interdisciplinary interactions will permit design changes to be made early in the design process and thereby increase the probability of meeting all customer requirements. Methods with a rapid turnaround capability will reduce design cycle time so that designers can explore a wide spectrum of alternatives within the schedule and cost constraints of a typical product development program. This will permit the U.S. aerospace industry to conduct the extensive tradeoffs needed to produce optimal designs.

Presented as Paper 97-0646 at the AIAA 35th Aerospace Sciences Meeting, Reno, NV, 6–9 January 1997; received 8 October 1997; revision received 15 February 1999; accepted for publication 2 March 1999.

*Senior Engineer, Computational Fluid Dynamics, Flight Sciences Division. Member AIAA.
†Research Engineer II, National Science Foundation Research Center for Computational Field Simulation, Nichols Research, Inc., 1165 Porters Chapel Road, TL112. Senior Member AIAA.
‡Regent's Professor, School of Aerospace Engineering. Associate Fellow AIAA.
§Technical Fellow, Flight Sciences Division. Associate Fellow AIAA.

A typical distributed computer environment is a mixture of several platforms that include single-user graphics workstations, mainframes, scalar and vector supercomputers, loosely coupled workstation clusters, and tightly coupled massively parallel processors (MPPs). It is becoming increasingly clear that the U.S. industry is migrating toward such an environment; however at this stage, it is not completely obvious as to what particular combination of platforms offers the most cost-effective means of meeting the demands of the design processes. The relative merits of different parallel computing environments needs to be investigated. Also, benefits of the parallel systems for multidisciplinary analysis using advanced methods such as ENSAERO relative to the conventional supercomputers that permit only a serial mode of operation need to be evaluated. The potential for significant improvements has been previously demonstrated by Byun and Guruswamy.[1]

Our primary technical objective is to develop an aeroservoelastic analysis capability that is fast, accurate, and cost effective. The ENSAERO code,[1,2] developed by Byun and Guruswamy at NASA Ames Research Center (NASA ARC), is state of the art and offers many features that make it ideally suited for the present research effort. These features include modular architecture; advanced fluid, structures, and controls analysis modules; clearly demonstrated capabilities for wing and wing–body configurations; and implementation on serial and parallel computers. Areas needing enhancements can be broadly divided into two categories. In the first category are items related to the analysis process itself, for example, improved visualization. The second category relates to improvements in the constituent modules, for example, implementing a more robust moving grid capability.

ENSAERO Solver Description

ENSAERO is a multidisciplinary aeroelastic code based on Euler/Navier–Stokes equations coupled with structural equations. ENSAERO has time-accurate methods based on both central difference and upwind schemes.[1,2] Baldwin–Lomax and Johnson–King turbulence models are included for viscous flows. For modeling

structures, the modal or finite element equations are used. An aeroelastic shape-conforming moving grid is used to include the effect of structural deformations on unsteady flows about wing and wing–body configurations. The code also has a builtin Fourier analysis module for unsteady flow postprocessing. The constituent parts of the parallel code, communicate with each other via the message passing interface (MPI).[3] ENSAERO has a modular architecture, so that different numerical schemes from different disciplines (as well as any one discipline) can be adopted very easily. The code is operational on a variety of platforms ranging from Cray-class vector computers to Intel iPSC/860 and IBM SP2-type distributed-memory parallel computers. It has been successfully applied to 1) perform steady, unsteady, and aeroelastic analysis of wing and wing–body configurations; 2) simulate control surface motion on wing and wing–body configurations including active control for flutter suppression; and 3) model steady flows on rigid full-aircraft configurations.

Code Enhancements

To improve the accuracy, robustness, and portability of ENSAERO on parallel systems, several enhancements are being made to the modular software. This work is ongoing, and to date enhancements for the code include the following.

1) To facilitate postprocessing, the pV3 visualization package,[4] which was developed at the Massachusetts Institute of Technology, has been integrated in the ENSAERO framework. The pV3 package provides an interactive tool for visualizing unsteady data as they become available during a flowfield computation. The pV3 is designed so that it can plug into a calculation from a local graphical workstation (the server) as the solver is executing on a remote set of heterogeneous processors (the clients). This allows the user to visualize data as the solution advances in time while pV3 performs most of the additional work required for visualization on the very same platforms that are generating the data. In this way, only small-size drawing primitives are transferred to the scene rendering hardware, thus avoiding communication bottlenecks and having to deal with large datasets locally.

2) A highly portable version of the ENSAERO code for parallel computing systems was developed. The code was modified so that it can be run using both MPI and the parallel virtual machine (PVM)[5] protocol on several platforms ranging from single-user graphics workstations to scalar and vector supercomputers to tightly coupled MPPs. The PVM version of the ENSAERO code has been developed in a manner that retains full MPI functionality while adding PVM protocols to enhance portability.

3) To allow multiblock H–H topology structured-grid generation for wing/body/tail configurations, the complete aircraft mesh program (CAMP),[6] a U.S. Air Force Wright Research Laboratory software, has been integrated into the ENSAERO framework.

4) The computational fluid dynamics module of ENSAERO has been modified to include appropriate boundary conditions to specify fan-face inflow and nozzle outflow conditions.

5) To reduce the turnaround time of a full aeroelastic analysis, an unstructured-grid fluids module[7] is currently being incorporated into the ENSAERO framework.

Test Case Geometries and Grids

Arrow-Wing Body

This was an example test case[8] that was supplied by NASA-ARC with the release of the parallel version of ENSAERO. In addition, a steady-state Navier–Stokes solution restart file generated on the NASA IBM SP2 system using the MPI protocol at $M = 0.85$ and $\alpha = -1$ deg was made available. As shown in Fig. 1, the configuration has a thin wing with a leading-edge sweep of 71.2 deg, a taper ratio of 0.1, and aspect ratio of 1.65. The wing is flat with a rounded leading edge and is mounted below the centerline of a slender body. The H–H grid topology for Navier–Stokes computations contains eight zones of 56 × 30 × 40 grid points each, for a total of 537,600 grid points (overall 110 points in the streamwise direction, 116 points in the spanwise direction, and 40 points normal to the body surface). The body is extended to the downstream boundary. Figure 2 shows the arrow-wing body field grid.

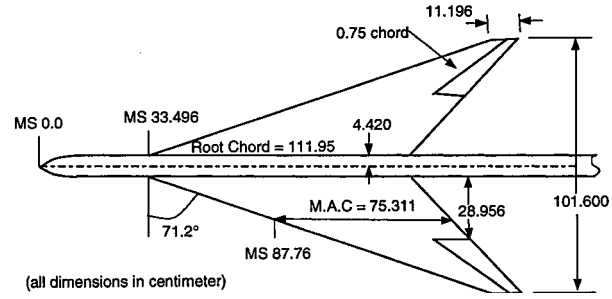

Fig. 1 Arrow-wing body configuration.

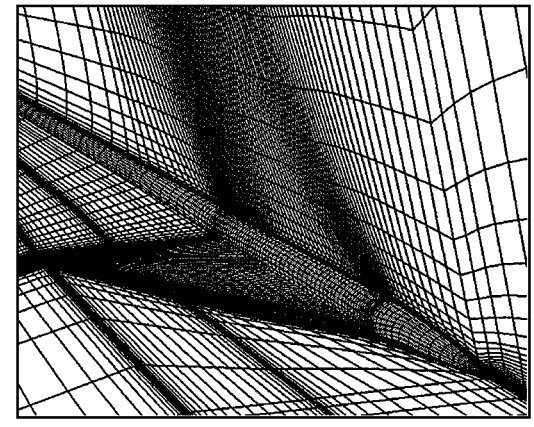

Fig. 2 Arrow-wing body field grid.

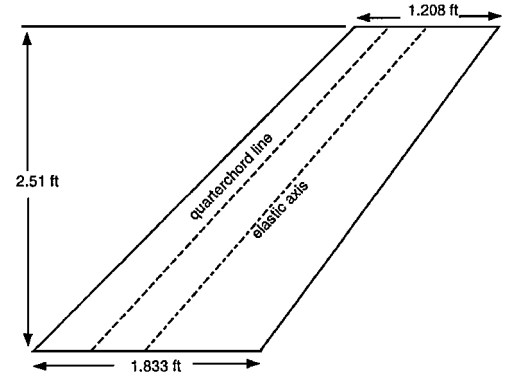

Fig. 3 AGARD wing 445.6 geometry.

AGARD Wing 445.6

This geometry is a standard aeroelastic configuration specifically designed for dynamic aeroelastic response.[9] This first AGARD aeroelastic configuration was tested in the 16-ft transonic dynamic tunnel (TDT) at the NASA Langley Research Center.[9,10] As shown in Fig. 3, the wing has a quarter-chord sweep angle of 45 deg, a panel aspect ratio of 1.6525, a taper ratio of 0.6576, and a NACA65A004 symmetric airfoil section in the streamwise direction. Full span and semispan models were tested in the TDT. The model used for this study is a semispan, wall-mounted model. To reduce the stiffness, holes were drilled through the maghogany wing. To ensure that the aerodynamic shape of the original wing was preserved, these holes were filled with rigid foam plastic. Flutter data for this model tested in air are available[9,10] over a range of Mach numbers from 0.338 to 1.141.

For the ENSAERO computations, C–H-type computational grids for both Euler and Navier–Stokes calculations contain 193 × 65 × 41 points with 193 points wrapped around the wing and the wake

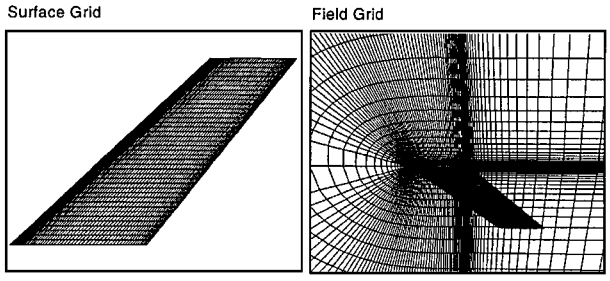

Fig. 4 Wing surface and plane-of-symmetry grid on AGARD wing 445.6.

(129 points on the wing surface), 65 points distributed from the wing root to the spanwise boundary (41 points on the wing surface), and 41 points distributed radially from the wing surface to the outer boundary. A properly clustered grid to resolve the boundary layer was ensured by forcing y^+ to be of order 1 for the cell next to the wall. Figure 4 shows the surface and field Euler grid. The Euler and Navier–Stokes grid topologies are similar to the grids used by Lee-Rausch and Batina.[11,12] In those works, a grid study was performed for the steady-state viscous flowfields by looking at an additional finer Navier–Stokes mesh of approximately 1.4×10^6 grid points identical in topology to the $193 \times 65 \times 41$ mesh. After some investigation with different grid densities, the $193 \times 65 \times 41$ mesh with 0.51×10^6 points was found to predict very similar steady-state surface pressure distributions as the finer mesh for $M = 0.96$ and for $M = 1.141$. Surface pressure plots also indicated that the coarser grid resolves the flow features across the span of the wing at least as well as the finer grid.

Results and Discussion

Arrow-Wing Body

To validate the PVM modified version of ENSAERO, computed steady solutions of the modified code are compared with those of the MPI original code for the arrow-wing body benchmark case. Accuracy and runtimes of the PVM and MPI versions were compared to assess the accuracy of the enhanced PVM version and the computational performance of both the PVM and MPI protocol on several platforms.

At the same conditions of $M = 0.85$ and $\alpha = -1$ deg, steady-state Navier–Stokes calculations are done and compared using a NASA SGI (NASSGI) workstations cluster (4 machines) with PVM, a Lockheed Martin SGI Power Challenge System (LMPC) with PVM, a Numerical Aerospace Simulation (NAS) Facility SGI Power Challenge Cluster (NASPC) with PVM and MPI, and a NASA IBM SP2 (SP2) with PVM and MPI. For the NASSGI, two processes were started on each of the four machines used so that each of the eight zones in the grid system was assigned to one process. This is functionally equivalent to using a different processor for each zone. On the LMPC shared-memory system and on the NASPC, each of the eight zones in the grid system was assigned to one processor. On the SP2, the sample case was run on eight nodes.

The residual histories for all zones were compared on each of the four parallel computing systems. The results indicated that the MPI and PVM versions of the code are producing identical results. As an example, Fig. 5 shows the residual histories of zones 3 and 7 for the NASPC.

The performances of the ENSAERO code running under MPI and PVM protocols were compared on the NASPC and the SP2. Figure 6 shows the comparison of MPI and PVM run time for steady solutions performance on the NASPC (1000 steps) and the SP2 (5000 steps). On both systems, the PVM version is slightly faster then the MPI version. Our results indicated that this difference in runtimes is due to the different communications overhead for both systems.

In Table 1, the performance of the PVM version of the code is compared on four parallel systems on the basis of wall clock time per step, total CPU time per step, and total CPU time per step per grid point. The data are based on the steady-state solutions for the arrow-wing body test case with a 537,600-point grid divided into eight equal-size zones. With a single-processor Cray C-90 CPU time per step per grid point of 5 μs, it is estimated that an 18 node SP2 (with an 18 zone grid and assuming linear speedup) will match single-processor C-90 performance.

Table 1 ENSAERO performance comparison on four parallel computing systems

Parallel computing system	No. compute nodes	Wall clock time/step, s	Total CPU time/step, s	Total CPU time/step/ grid point, μs
NASSGI	4	70.2	562	1045
LMPC	8	9.12	73	136
NASPC	8	8.84	71	132
SP2	8	6.12	49	91

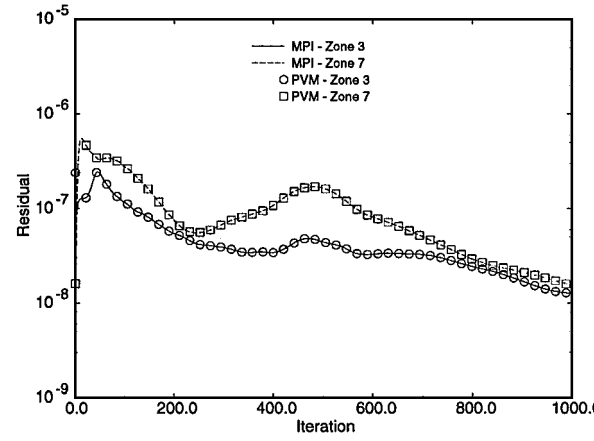

Fig. 5 Residual histories for zones 3 and 7 of the eight-zone arrow-wing body test case on NASASGI for PVM and MPI runs.

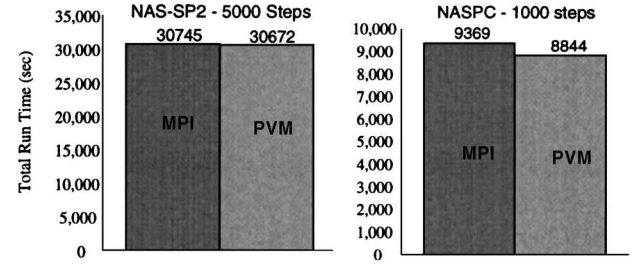

Fig. 6 Comparison of MPI and PVM run time performance on NASPC (1000 steps) and on SP2 (5000 steps).

AGARD Wing 445.6

To assess the level of accuracy of the enhanced ENSAERO code, it was further validated by correlating ENSAERO solutions with available measured/computed[9–12] data for the AGARD wing 445.6 that was specifically designed for code validation. Wing geometry data, modal properties, and flutter data for air were assembled for two cantilever-mounted models of different properties: weak3 and solid2. Of these two models, the weak3 model has been the focus of computational elasticity efforts because available data cover a wide range of Mach numbers. Based on experimental and computational data available, ENSAERO aeroelastic time integration calculations were performed for the weak3 model at $M = 0.96$ and 1.141 and $\alpha = 0$ deg in air. In Ref. 12 computations of the flutter boundary for this geometry using CFL3D indicated that Euler calculations were in good agreement in flutter characteristics for freestream Mach numbers below unity. For freestream Mach numbers above unity, the computed aeroelastic results predicted a premature rise in the flutter boundary as compared with the experimental boundary. In later work by Lee-Rausch and Batina,[11] effects of fluid viscosity, structural damping, and the number of modes in the structural model were investigated. Navier–Stokes time-marching calculations were

performed at a freestream Mach number of 1.141, and they indicated that the fluid viscosity has a significant effect on the supersonic flutter boundary for this wing, whereas the structural damping and number of modes in the structural model have a lesser effect. Based on these results, for this work, an Euler time-integration calculation was done at $M = 0.96$ and a Navier–Stokes time-integration flutter calculation at $M = 1.141$.

To initialize a dynamic aeroelastic analysis, static solutions were obtained first. Because this wing has a symmetric airfoil, there are no static aeroelastic deflections at $\alpha = 0$ deg. Therefore, steady rigid solutions at $M = 0.96$ and 1.141 at $\alpha = 0$ deg was used as the starting solution for the corresponding dynamic aeroelastic analysis at $M = 0.96$ and 1.141, respectively. For steady-state calculations, convergence criteria included three orders of magnitude reduction in residual and no variation in the first three significant digits of the integrated force values. This required approximately 4000 cycles. For the Euler calculation, the finite difference scheme was used, and for the Navier–Stokes computations, the upwind scheme was used at experimental flutter conditions, which corresponds to a freestream Reynolds number of 5.377×10^5/ft. These steady-state flowfields are used as initial conditions for the unsteady calculations.

Comparisons of ENSAERO and CFL3D steady-state pressure coefficient contours on the upper wing surface at $M = 0.96$ and 1.141 are shown in Figs. 7 and 8, respectively. The basic flow characteristics of the ENSAERO Euler and Navier–Stokes solutions match well with the CFL3D computations. These solutions provided the starting point for the dynamic aeroelastic analysis using four mode shapes for which oblique projections are shown in Fig. 9. The modes represent first bending, first torsion, second bending, and second torsion as calculated by a finite element analysis.[8] The modes have natural frequencies ranging from 9.6 Hz for first bending mode to 91.54 Hz for second torsion mode.

Time-integration calculations were performed to determine the flutter characteristics of this configuration at $M = 0.96$ and 1.41 at $\alpha = 0$ deg. To capture the flutter point, the dynamic aeroelastic computations were performed at several values of q. At each q, the calculation was stopped when aeroelastic transients were computed for at least two cycles in the lowest frequency (first bending) mode. This required between 18,000 and 22,000 time steps (based on a conservative physical time step of $5.0E-06$ s) depending on q. For $M = 0.96$, calculations were done at $q = 100$, 111, 123, and 147% of the experimental value (0.425 psi for Mach = 0.96) to bracket the flutter point. Similarly, for $M = 1.141$, calculations were done at $q = 160$, 180, and 210% of the experimental value (0.712 psi for $M = 1.141$). When using Navier–Stokes equations, a freestream Reynolds number must be specified at each dynamic pressure of interest. When comparing with experimental data, this means that, in theory, the Reynolds number needs to be adjusted for each q. Lee-Rausch and Batina[11,12] performed viscous time-marching calculations with and without a variation in the freestream Reynolds number for a variation of q. The flutter results were independent of this change (less than 1% difference). Based on these results, the Navier–Stokes time-marching calculations for this work were performed at the experimental flutter value of Reynolds number for each q. The motion of the wing was initiated by applying a small initial velocity to all four modes in each of the dynamic calculations. No structural damping was introduced into the system. Figure 10 shows the time history of the generalized displacements for each mode at $q = 0.625$ psi and $M = 0.96$. Figure 11 shows the time history of generalized displacements of the first mode for a range of q between 0.425 and 0.625 psi at $M = 0.96$. At $q = 0.425$ psi, there is enough damping in the system to maintain stability. At $q = 0.625$ psi the time history of the generalized displacements indicates that the wing is dynamically unstable, and flutter occurs. Similar results were obtained when plotting the time history of the generalized displacements at $M = 1.141$ at the onset of flutter at $q = 1.5$ psi.

The computed flutter dynamic pressure and frequency were determined by interpolating the dynamic pressures and the computed frequencies to find the value at zero damping of the flutter mode. Figure 12 shows a comparison of the Euler and Navier–Stokes flutter

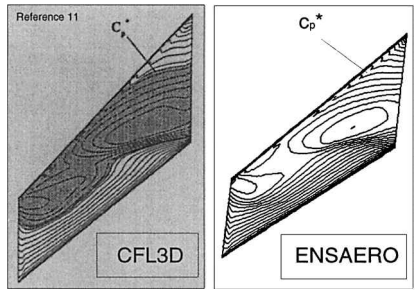

Fig. 7 Comparison of CFL3D and ENSAERO steady-state pressure coefficients at $M = 0.96$ for AGARD wing 445.6.

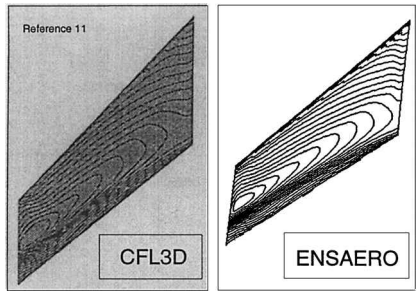

Fig. 8 Comparison of CFL3D and ENSAERO steady-state pressure coefficients at $M = 1.141$ for AGARD wing 445.6.

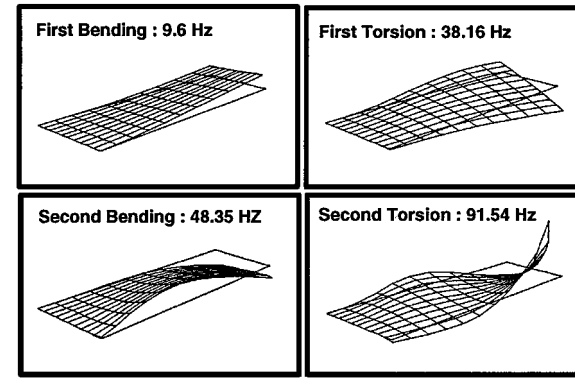

Fig. 9 Free-vibration mode shapes for AGARD wing 445.6.

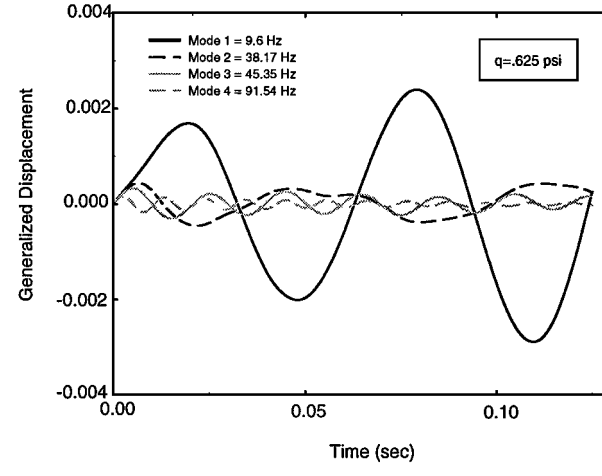

Fig. 10 Time history of generalized displacements of all modes at $M = 0.96$ and $q = 0.625$ psi for AGARD wing 445.6.

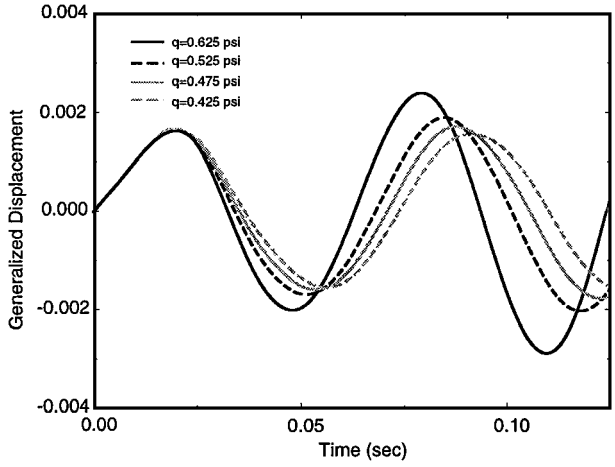

Fig. 11 Time history of generalized displacement of the first mode at $M = 0.96$ for AGARD wing 445.6.

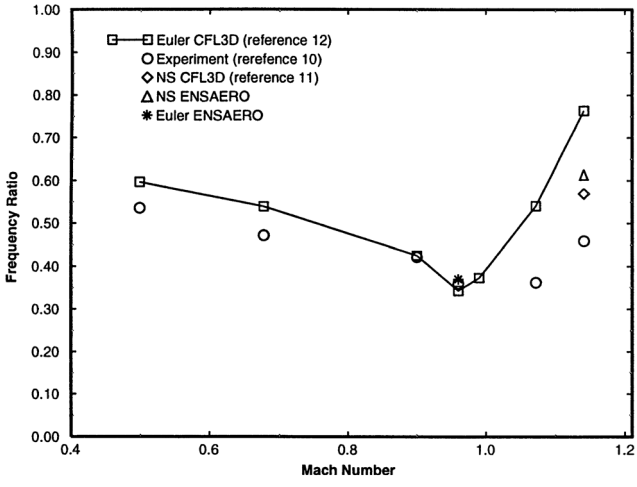

Fig. 12 ENSAERO Euler and Navier–Stokes flutter predictions compared to experimental data and CFL3D computational results.[11,12]

predictions of flutter frequency by ENSAERO with experimental data and CFL3D solutions for wing 445.6. Flutter frequency here is defined as the ratio of the frequency associated with the first bending mode of the aeroelastic response to the uncoupled natural frequency of the first torsion mode. The experimental data show a typical transonic flutter dip with the bottom near $M = 1.0$. CFL3D Euler flutter predictions match the experimental flutter frequency closely for Mach numbers below unity. The ENSAERO flutter frequency at $M = 0.96$ matches the experimental and CFL3D results well. However, at freestream Mach numbers above unity, the computed CFL3D Euler solutions predict a premature rise in the flutter boundary. It is clear that modeling the boundary layer at $M = 1.141$ improved the correlation with the experiment; however, the flutter characteristics predicted by a Navier–Stokes time-marching analysis for both CFL3D and ENSAERO are still high in comparison with experimental solution. The loss of accurate tip geometry definition in the computational geometry and the accuracy of the modeling of the boundary layer could play a significant role in the overprediction of both ENSAERO and CFL3D for Mach numbers above unity. These issues were also raised in the work by Lee-Rausch and Batina[11] and will need to be addressed in future work.

The multiblock AGARD wing 445.6 test problem also provides a good illustration of the capabilities of the parallel code. To demonstrate code scalability, that is, impact of varying the number of processors on computational performance, the grid was divided in 2, 4, 6, 8, and 16 subgrids. The domain was decomposed by splitting the grid at spanwise locations and assigning the same number of

Table 2 ENSAERO performance for AGARD wing 445.6 flutter analysis using MPI on the SP2 parallel computing system

No. compute nodes	Wall clock time/step, s	Total CPU time/step, s	Total CPU time/step/ grid point, μs
2	32.5	65	127
4	15.9	63	123
8	8	64	124
16	4.1	65	127

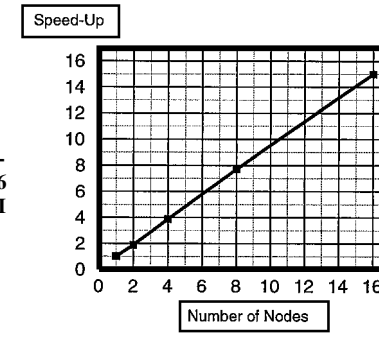

Fig. 13 ENSAERO speed-up for AGARD wing 445.6 flutter analysis using MPI on the SP2.

grid points to each block. Each block was then solved on a separate node on the SP2 system. Table 2 shows the ENSAERO performance for AGARD wing 445.6 flutter analysis using MPI on SP2. Good actual scalability compared to theoretical scalability was produced. Figure 13 shows the speedup as the number of nodes is increased. Almost linear speedup was observed.

Conclusions

The results presented represent the initial phase in the development and validation of a fast, accurate, and cost-effective aeroservoelastic method on advanced parallel computing systems. A highly portable version of the ENSAERO code capable of running on a wide variety of platforms using both PVM and MPI has been developed. A visualization package and a multiblock H–H topology structured grid generator have been incorporated in the ENSAERO framework the modified code has been successfully run on several parallel computing systems ranging from distributed-memory SP2 to shared-memory SGI Power Challenge. Verification runs were done on an arrow-wing body geometry, and the results showed that the enhanced code performs according to the specifications. Flutter calculations on the AGARD wing 445.6 showed a close agreement of steady-state pressures and flutter frequency to CFL3D computational results in the transonic Mach number range. The computations at $M = 0.96$ matched the experimental data well, however at $M = 1.141$ the ENSAERO results, like the CFL3D results, predict a premature rise in the flutter boundary. Initial data on scalability and code performance indicate that the code scales almost linearly up to 16 processors for aeroelastic computations.

This work will produce the knowledge base urgently needed by U.S. industry to make informed decisions about where and how to apply the computational aerosciences and high-performance computing technologies for maximum payoff in design and development of advanced subsonic transports of the future. The upgraded ENSAERO capability will significantly enhance aerodynamic loads and flutter analysis methodologies crucial to achieving optimal structural design while meeting desired performance goals.

Acknowledgments

This research was performed under the NAS2-14092 Contract sponsored by NASA Ames Research Center (NASA ARC) with G. P. Guruswamy as the Technical Monitor. Thanks are due to G. P. Guruswamy of NASA ARC and C. Byun of MCAT, Inc., for their support and counsel. The use of NASA ARC IBM SP2 system and SGI workstation cluster is gratefully acknowledged.

References

[1]Byun, C., and Guruswamy, G. P., "A Comparative Study of Serial and Parallel Aeroelastic Computations on Wings," NASA TM 108805, Jan. 1994.

[2]Guruswamy, G. P., "User's Guide for ENSAERO—A Multidisciplinary Program for Fluid/Structural/Control Interaction Studies of Aircraft (Release 1)," NASA TM 108853, Oct. 1994.

[3]Dongarra, J., Hempel, R., Hey, A., and Walker, D., "A Proposal for a User-Level, Message Passing Interface in a Distributed Memory Environment," Oak Ridge National Lab., TM-12231, June 1993.

[4]Haimes, R., "pV3: A Distributed System for Large-Scale Unsteady CFD Visualization," AIAA Paper 94-0321, Jan. 1994.

[5]Beguelin, A., Dongarra, J., Geist, A., Mancheck, R., and Sunderam, V., "A User Guide to PVM Parallel Virtual Machine," Oak Ridge National Lab., TM-11826, March 1992.

[6]Schuster, M. D., Vadyak, J., and Atta, E., "Static Aeroelastic Analysis of Fighter Aircraft Using a Three-Dimensional Navier–Stokes Algorithm," *Journal of Aircraft*, Vol. 27, No. 9, 1990, pp. 820–825.

[7]Bhat, M. K., and Parikh, P., "Development of an Unstructured Grid Fluids Module for ENSAERO in a Parallel Environment," *Computational Aerosciences Workshop by the High Performance Computing and Communications Program*, NASA CD Conf. Pub. 20011, Aug. 1996.

[8]Obayashi, S., Chiu, I. T., and Guruswamy, G., "Navier–Stokes Computations on a Full Wing–Body Configuration with Oscillating Control Surfaces," *Journal of Aircraft*, Vol. 32, No. 6, 1995, pp. 1227–1233.

[9]Yates, E. C., "AGARD Standard Aeroelastic Configurations for Dynamic Response. Candidate Configuration I.-Wing 445.6," NASA TM 100492, Aug. 1987.

[10]Yates, E. C., Land, N. S., and Foughner, J. T., "Measured and Calculated Subsonic and Transonic Flutter Characteristics of a 45 deg Sweptback Wing Planform in Air and Freon-12 in the Langley Transonic Dynamics Tunnel," NASA TN D-1616, March 1963.

[11]Lee-Rausch, E. M., and Batina, J. T., "Wing Flutter Computations Using an Aerodynamic Model Based on the Navier–Stokes Equations," *Journal of Aircraft*, Vol. 33, No. 6, 1996. pp. 1134–1147.

[12]Lee-Rausch, E. M., and Batina, J. T., "Wing Flutter Boundary Prediction Using Unsteady Euler Aerodynamic Method," *Journal of Aircraft*, Vol. 32, No. 2, 1995, pp. 416–422.